

Electron capture in collisions between O^{6+} ions and H_2O molecules

D. Bodewits* and R. Hoekstra†

KVI Atomic Physics, University of Groningen, Zernikelaan 25, NL-9747 AA Groningen, The Netherlands

(Received 6 June 2007; published 6 September 2007)

By means of photon emission spectroscopy, state selective electron capture cross section for low energy (0.1–7.5 keV/amu) collisions of O^{6+} on H_2O molecules have been measured. Over the range of interaction energies the state selective cross sections change strongly, i.e., by factors up to 5, while the total one-electron capture cross section turns out to increase by approximately 40%. Possibilities of using O VI line emission ratios as a remote diagnostics of astrophysical plasma are indicated.

DOI: [10.1103/PhysRevA.76.032703](https://doi.org/10.1103/PhysRevA.76.032703)

PACS number(s): 34.70.+e, 96.25.Qr, 95.30.Dr, 95.85.Mt

I. INTRODUCTION

At keV/amu energies and below, interactions between multiply charged ions and neutrals are dominated by charge exchange processes. Electrons are captured into excited states that subsequently decay to the ground state through the emission of one or more photons and/or electrons. X-ray and extreme ultraviolet (euv) emission following electron exchange by solar wind minor ions has been found on a large variety of solar system objects, such as comets and planets, e.g., [1–4]. The line emission depends on the population of specific electronic states in the ions. The population of these states depends on the ion velocity and electron donor species. Therefore the line emission can be regarded as a fingerprint of the underlying charge exchange processes. Recently, comets have been used as the test beds for demonstrating the astrophysical diagnostic potential of charge exchange driven x-ray and euv emission following electron capture by solar wind minor ions [3–9].

Apart from protons and alpha particles, the solar wind contains a small percentage of multiply charged C, O, N, and Ne ions. In addition, very small fractions of intermediately charged Mg, Si, S, and Fe ions are present in the solar wind [10]. The solar winds can be divided in slow and fast winds at approximately 200–400 and 500–1000 km s⁻¹, respectively. The full velocity range encompassed by the slow and fast winds corresponds to a collision energy range of approximately 0.2–6 keV/amu.

The most abundant solar wind minor ion is O^{6+} , which has not been considered in great detail because its emission falls just below the low-energy detection limits of *Chandra* and *XMM-Newton*. O VI emission has been detected in fuse observations of the comet C/WM1 [11] and extreme ultraviolet explorer (EUVE) observations of comet Hyakutake [12]. Oxygen ions precipitating into the Jovian atmosphere are important contributors to the observed euv and x-ray emission of the aurorae of Jupiter [13]. Model calculations based on O^{q+} - H_2 interactions underline the important role of O^{6+} ions as line emitters [14,15].

In particular, state selective electron capture by O^{6+} in collisions on H, H_2 , and He has been studied extensively,

e.g., in Refs. [15–21]. For many typical cometary and planetary target species such as CO, CO_2 , and H_2O the availability of experimental or theoretical data is very limited [22–24].

In this paper we will focus on the one-electron capture in 0.1–7.5 keV/amu collisions of O^{6+} on H_2O molecules. Water molecules are the most likely electron donors in the interaction of the solar wind with comets.

II. EXPERIMENT

The experimental data were taken with the Photon Emission Spectroscopy (PES) setup installed at the KVI (University of Groningen) (see, e.g., [20,25]). Highly charged ions from the Electron Cyclotron Resonance Ion Source are guided into the reaction chamber, where the ion beam is focused and decelerated by an ion-optical lens system, similar to the one used before [26,27]. The lens system allows for extending the range of direct beam energies from 2–24q keV down to 0.3q keV. In the reaction chamber within the last lens element, the ions collide with a supersonic neutral gas jet of approximately 2 mm diameter.

The water vapor jet was prepared especially to avoid contamination dissolved in the water. A reservoir filled with demineralized water was repeatedly cooled with liquid nitrogen and then pumped to remove residual air molecules [28].

Charge exchange emission from the collisions is observed with a grazing incidence spectrometer sensitive in the 10–40 nm range. This spectrometer is equipped with a position sensitive multichannel plate detector, allowing for the simultaneous observation of a wavelength window of approximately 10 nm. The sensitivity of the spectrometer was calibrated by means of charge exchange reactions of which absolute cross sections are known.

Figure 1 shows typical spectra obtained at different collision velocities. With the 1200 grooves/mm grating used for this experiment, the resolution of the spectrometer is approximately 0.3 nm full width at half maximum. Spectra were measured at two different positions along the Rowland circle, in order to obtain first and second order spectra. In second order, the spectrometer is less sensitive, but the $1s^24d-1s^22p$ and $1s^24s-1s^22p$ peaks that overlay in first order are clearly separated.

*bodewits@kvi.nl

†hoekstra@kvi.nl

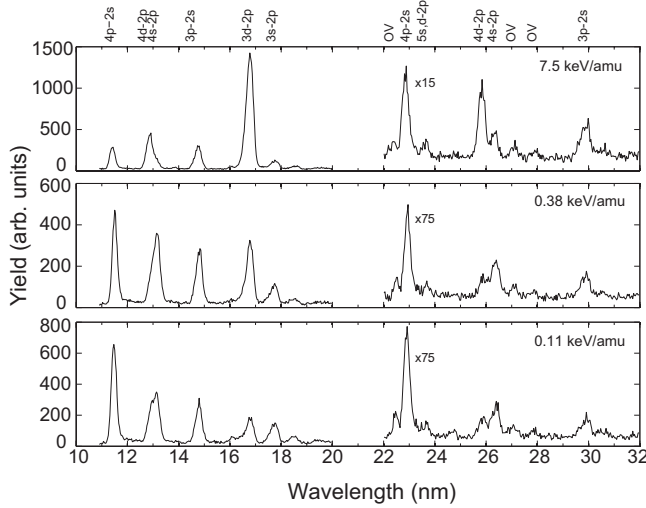


FIG. 1. Velocity dependence of charge exchange spectra for collisions between O^{6+} and H_2O . Shown are the first order (10–20 nm) and the second order (22–32 nm) spectra for collision energies of 7.5 keV/amu (top), 0.38 keV/amu (middle), and 0.11 keV/amu (bottom). The spectra are corrected for the accumulated charge and target pressure, but not for the spectrometer's wavelength dependent response. Second order spectra are blown up for the ease of presentation.

III. SPECTRAL ANALYSIS

All spectra were analyzed by fitting Gaussian peaks to the data. Emission cross sections were deduced from photon yields by using the following relation:

$$\sigma_{em} = AS(\lambda) \frac{q}{Q} N, \quad (1)$$

where $S(\lambda)$ is the spectrometer's wavelength dependent response, q is the charge state of the incoming ion, Q is the accumulated charge, N is the photon yield. A includes all parameters that are kept constant during our experiments, among which is the target density, and is found by calibrating via known cross sections for $He^{2+} + H_2O$ [29,30].

In order to derive population cross sections from the measured line emission cross sections, the line emission cross sections should be corrected for branching ratios and cascade effects. The decay scheme of $O\ VI$ is given in Fig. 2. Transitions from $n=4 \rightarrow 3$ fall outside the wavelength range accessible to the spectrometer when equipped with the 1200 G/mm grating used here. Transitions from $n=5 \rightarrow 2$ fall within the observable wavelength regime, but lie too close to the strong $4p-2s$ transition to be resolved in first order. In second order however, the separation between the lines becomes large enough for individual detection and careful inspection of these spectra shows a weak emission feature near 23.5 nm due to the $5s, 5d-2p$ transitions at ~ 11.7 nm (see Fig. 1). As the combined strengths of the $5s, 5d-2p$ transitions is $\sim 10\%$ of the $4p-2s$, we will assume that capture into $n=5$ is weak and to first order negligible. The population cross sections can therefore be derived from

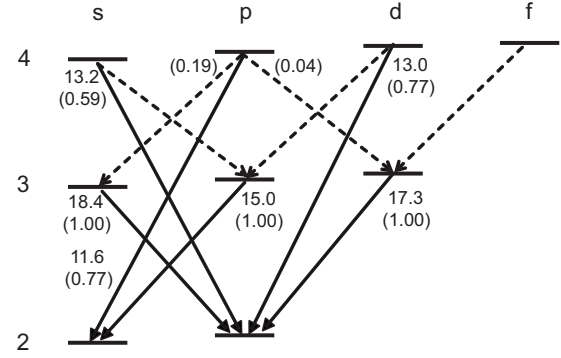


FIG. 2. Grotrian diagram of $O\ VI$ ($1s^2nl$). Observed transitions are indicated with solid lines, other transitions by dashed lines. Wavelengths are given in nanometers, the numbers between brackets are the branching ratios.

the measured line emission cross sections by means of the following relations:

$$\sigma(4s) = \sigma_{em}(13.2)/0.59,$$

$$\sigma(4p) = \sigma_{em}(11.6)/0.77,$$

$$\sigma(4d) = \sigma_{em}(13.0)/0.77,$$

$$\sigma(3s) = \sigma_{em}(18.4) - 0.19\sigma(4p) = \sigma_{em}(18.4) - 0.25\sigma_{em}(11.6),$$

$$\begin{aligned} \sigma(3p) &= \sigma_{em}(15.0) - 0.41\sigma(4s) - 0.23\sigma(4d) \\ &= \sigma_{em}(15.0) - 0.69\sigma_{em}(13.2) - 0.30\sigma_{em}(13.0), \end{aligned}$$

$$\sigma(3d + 4f) = \sigma(17.3) - 0.04\sigma(4p) = \sigma(17.3) - 0.03\sigma_{em}(11.6). \quad (2)$$

From these relations, it is clear that except for the $4f$ state, capture into the $n=4$ states is observed directly, and that population cross sections for $n=3$ are derived indirectly from the line emission cross sections. It is not possible to separate capture into the $1s^23d$ and $1s^24f$ states without observing the direct transition between those two states at longer wavelengths.

The results are subject to a number of uncertainties. The dominating absolute uncertainty is that arising from the spectrometer's calibration. The calibration was obtained by means of cross sections for charge exchange emission from He^{2+} ions following the procedures described in Hoekstra and co-workers [25,26] and Dijkkamp *et al.* [16] and for H_2O has a demonstrated accuracy of approximately 20% [30]. This error affects all data points, and leads to a simple scaling factor. A more complex error is due to the uncertainty in the wavelength dependent sensitivity of the spectrometer, which is in the order of 10–15%. Added in quadrature these uncertainties lead to an absolute systematic uncertainty of 25%. The uncertainty associated with the wavelength-dependent sensitivity may also influence the relative line strengths which are of importance when assessing cascade contributions. Target fluctuations were controlled by performing regular calibration measurements, but lead to a ran-

TABLE I. Fit results: measured emission cross sections for one electron capture in O⁶⁺+H₂O collisions, for different collision energies. All cross sections are in units of 10⁻¹⁶ cm². Only relative errors are given. The systematic uncertainty is approximately 25%.

| E (keV/amu) | 11.6 nm | 13.0 nm | 13.2 nm | 15.0 nm | 17.3 nm | 18.4 nm |
|---------------|---------|---------|---------|---------|---------|---------|
| 0.11 | 11±1.1 | 3.2±0.3 | 5.4±0.5 | 4.2±0.4 | 5±0.5 | 2.6±0.3 |
| 0.19 | 8.7±0.9 | 3.2±0.3 | 5.3±0.5 | 4.4±0.4 | 8±0.8 | 2.1±0.2 |
| 0.38 | 7.3±0.7 | 2.8±0.3 | 5.3±0.5 | 4.2±0.4 | 10±1.0 | 1.7±0.2 |
| 1.31 | 5.0±0.5 | 3.0±0.3 | 4.1±0.4 | 3.1±0.3 | 12±1.2 | 1.2±0.1 |
| 3.94 | 4.3±0.4 | 4.5±0.5 | 2.9±0.3 | 3.6±0.4 | 22±2.2 | 1.3±0.1 |
| 7.50 | 3.3±0.3 | 4.7±0.5 | 1.4±0.1 | 3.2±0.3 | 33±3.3 | 1.3±0.1 |

dom error in the order of 5%. Statistical errors for these experiments were small due to high photon yields and never exceeded 1% (1 σ). Therefore we assume a relative uncertainty of 10% in the line emission cross sections.

The measured line emission cross sections and the derived state selective cross sections are presented in Tables I and II.

IV. RESULTS AND DISCUSSION

A. Population cross sections

The state selective cross sections, determined from the line emission data via Eq. (2), are shown in Fig. 3. Cross sections for electron capture into the 1s²3s and 1s²3p states are very small ($\leq 10^{-16}$ cm²). Therefore although we did not measure separate 1s²4f and 1s²3d cross sections, it seems very reasonable to assume that capture into 1s²3d is not significant and thus that $n=4$ is the dominant reaction channel in collisions between O⁶⁺ and H₂O molecules. This is in line with the translational energy spectroscopy (TES) experiments by Seredyuk *et al.* [31] and with predictions by the classical over-the-barrier model [32]; see Fig. 4. In this figure, the reaction windows for electron capture at velocities of 0.25 and 4 keV/amu are shown. The reaction window can be seen to be positioned between the $n=4$ and $n=5$ states of O VI. Capture into $n=4$ occurs almost resonantly and can therefore to be expected to be the main capture channel. From the position of the reaction window, capture into $n=3$ seems very unlikely.

At low energies, the 1s²4p-1s²2s transition at 11.6 nm is the strongest line in the spectrum, followed by the relatively

strong 1s²4s-1s²2p emission. Around 0.5 keV/amu, all emission lines in the spectrum are roughly equally strong, as are the capture cross sections. At high velocity, the spectrum is completely dominated by the 1s²3d-1s²2p transition at 17.3 nm, implying that the ℓ -state distribution has shifted to higher states.

The population of low ℓ states at low energy, and a near statistical distribution at higher energy, is a general feature in electron capture by multiply charged ions (see, e.g., [33,34]). To illustrate the change in the ℓ distribution more qualitatively, two measured fractional populations of the 4 ℓ states are shown in Fig. 5. At the lowest velocity, there is a fair agreement with the distribution function predicted for electron transfer via purely radial coupling [35,36]. At the highest velocity, where rotational couplings are important, the ℓ -state distribution roughly resembles a statistical distribution ($2\ell+1$), but the 4f state seems to be overpopulated with respect to the other 4 ℓ states.

To some extent, as rotational coupling is linked to the collisional angular momentum, the shift in the ℓ -state distribution over angular momenta may be understood in terms of the classical over-the-barrier model [37]. In the frame of the O⁶⁺ ion, the target has an apparent angular momentum L of the order $L=bv_p$, with b the impact parameter and v_p the projectile velocity. The maximum impact parameter is the capture radius R_c at which the electron can cross the potential barrier between the target and projectile. For O⁶⁺ on H₂O, this radius is 12.7 a.u. (Table III). The maximum (non-integer) angular momentum ℓ of the captured electron can then be estimated using the relation $L^2=\ell(\ell+1)$. Capture into $\ell=3$ becomes possible at collision energies of approxi-

TABLE II. State selective cross sections for one electron capture in O⁶⁺+H₂O collisions, for different collision energies. All cross sections are in units of 10⁻¹⁶cm². Only relative errors are given. The systematic uncertainty is approximately 25%.

| E (keV/amu) | 3s | 3p | 4s | 4p | 4d | 4f+3d | Total |
|---------------|----------|----------|---------|---------|---------|---------|--------|
| 0.11 | 0.8±0.3 | -0.5±0.6 | 9.1±0.9 | 14±1.4 | 4.1±0.4 | 4.8±0.6 | 33±1.9 |
| 0.19 | 0.4±0.3 | -0.2±0.6 | 9.0±0.9 | 11±1.1 | 4.1±0.4 | 7.6±0.8 | 32±1.8 |
| 0.38 | 0.0±0.2 | -0.3±0.6 | 8.9±0.9 | 9.5±1.0 | 3.6±0.4 | 9.4±1.0 | 31±1.8 |
| 1.31 | -0.2±0.2 | -0.6±0.4 | 7.0±0.7 | 6.5±0.7 | 3.9±0.4 | 11±1.2 | 28±1.6 |
| 3.94 | 0.3±0.2 | 0.2±0.4 | 5.0±0.5 | 5.5±0.6 | 5.8±0.6 | 22±2.2 | 39±2.4 |
| 7.50 | 0.9±0.1 | 0.9±0.4 | 2.3±0.2 | 4.3±0.4 | 6.1±0.6 | 33±3.3 | 47±3.4 |

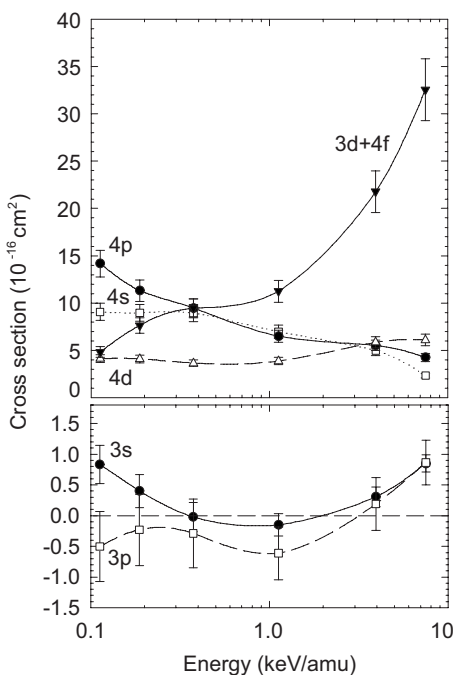


FIG. 3. Velocity dependence of state selective, single electron capture cross sections for $O^{6+}+H_2O$. Upper panel: Capture into $n=4$. \square : $\sigma(4s)$; \bullet : $\sigma(4p)$; \triangle : $\sigma(4d)$; \blacktriangledown : $\sigma(3d+4f)$. Lower panel: Capture into $n=3$. \bullet : $\sigma(3s)$; \square : $\sigma(3p)$. Lines are drawn to guide the eye. Only relative errors are given. The systematic uncertainty is approximately 25%.

mately 2 keV/amu, above which we indeed observe a steep increase in the $4f$ capture cross section (Fig. 3).

As the $4f$ population is determined from the $1s^23d-1s^22p$ transition, the apparent overpopulation of the $4f$ state at both low and high collision energies might be partly due to capture into the $3d$ and $5g$ states. As mentioned before, the measured $3s$ and $3p$ capture cross sections are close to zero

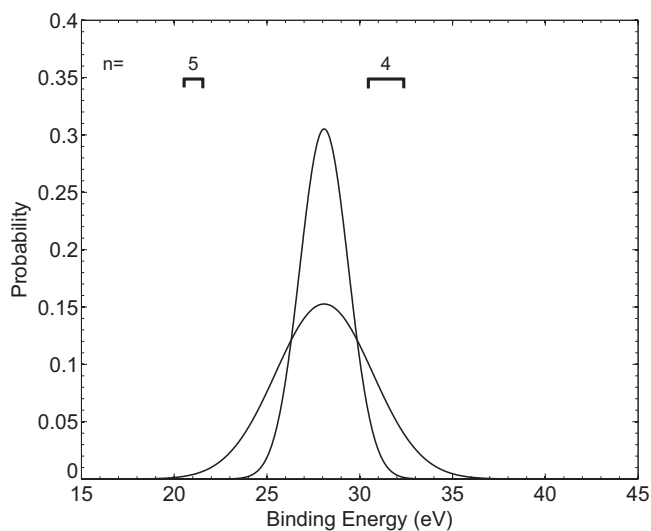


FIG. 4. Over-the-barrier predictions for one electron capture in $O^{6+}+H_2O$ collisions. Reaction windows for collision energies of 0.25 and 4 keV/amu. O VI states are indicated.

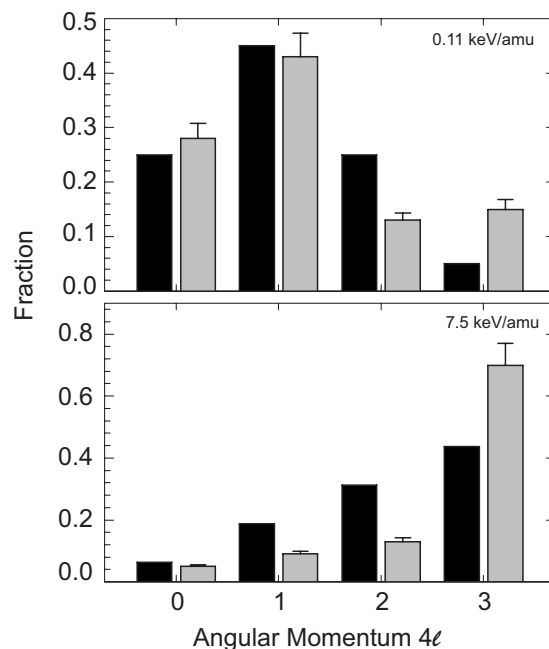


FIG. 5. Comparison of measured (gray) and theoretical distribution (black) over the 4ℓ states. Top panel: Measured distribution at 0.11 keV/amu, compared with a radial coupling determined low energy distribution [35,36]. Bottom panel: Measured distribution at 7.5 keV/amu, compared with a statistical ℓ distribution typical for higher collision velocities.

and therefore it seems logical that capture into $3d$ is also negligible. However, in their TES experiments at low energies (0.75–1.5 keV/amu) Seredyuk *et al.* [31] find that next to dominant capture into $n=4$, formation of $O^{5+}(n=3)$ through dissociative capture channels could be significant (up to 50%). Capture via these channels might therefore explain the apparent slight overpopulation of the $4f$ state at low energies. However, the contribution of these dissociative channels becomes smaller with decreasing velocity [31].

At higher velocities, the reaction window widens enough to allow for direct capture into $n=5$ (Fig. 4). Also, the higher velocities imply higher values of the electron’s angular momentum. The apparent overpopulation of $4f$ at the higher velocities may therefore be attributed to cascade contributions of the $5g$ state.

B. Total cross sections

By summing all our state selective cross sections, we determined velocity dependent, total one electron capture cross

TABLE III. Ionization potentials and resulting over-the-barrier predictions for capture distances and geometrical cross sections.

| n | IP_n (eV) | $R_{c,n}$ (a.u.) | σ_n (\AA^2) |
|-----|-------------|------------------|-------------------------------|
| 1 | 12.6 | 12.7 | 39 |
| 2 | 27 | 8.6 | 11 |
| 3 | ~ 45 | 6.9 | 21 |

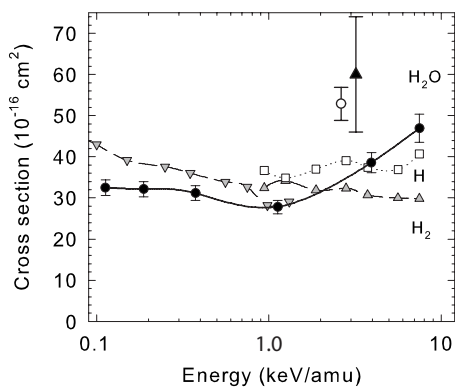


FIG. 6. Velocity dependence of total one electron capture cross sections for collisions between O⁶⁺ and H₂O, ●, compared with charge exchange cross sections for H₂ (△: [16]; ▽: [20]) and H (□: [16]). ○: Total charge changing cross section from [24]. ▲: Total charge changing cross section for C⁶⁺+H₂O [38]. Lines are drawn to guide the eye. Only relative errors are given. The systematic uncertainty is approximately 25%.

sections. The results are shown in Fig. 6. Above 1 keV/amu, where capture into $1s^24f$ becomes more and more important, the total cross section increases significantly. In the figure, total one electron capture cross sections for collisions with H and H₂ are also given for comparison. According to the classical over-the-barrier model, one electron capture cross sections scale with the inverse of the ionization potential of the target. The binding energy of water is 12.6 eV, that of H is 13.6 eV, and that of H₂ is 16.1 eV. The over-the-barrier model thus predicts that the one electron capture cross sections for all species will be of comparable magnitude, which is confirmed by our results.

Total charge changing cross sections for O⁶⁺+H₂O have recently been measured by Mawhorter *et al.* [24]. At a collision energy of 2.6 keV/amu, they measured a charge changing (O⁶⁺→O⁵⁺) cross section of $(53 \pm 4) \times 10^{-16}$ cm². A similar cross section has been measured for C⁶⁺+H₂O collisions [38]. These cross sections are much larger than the one electron capture cross sections determined by us at comparable energies, which by interpolation would be approximately $(34 \pm 8) \times 10^{-16}$ cm². The difference can only be explained by autoionizing double electron capture processes.

The over-the-barrier model [32] can be used to make a rough estimation of the multiple electron capture cross sections. Using binding energies from literature [39] and assuming the binding energy of the third electron to be approximately 45 eV, we find cross sections for one, two, and three electron transfer of $\sigma_1=39$, $\sigma_2=11$, and $\sigma_3=21 \times 10^{-16}$ cm²,

respectively (see Table III). The σ_1 agrees well with the single electron capture cross section we measured, while the sum of σ_1 and σ_2 is close to the aforementioned charge changing cross sections ($q=6 \rightarrow q=5$).

Following the argumentation of [40], it is estimated that two electron capture will mainly populate ($3\ell n' \ell', n'=5-7$) configurations. The resulting energy defects would coincide with the feature observed in the TES spectra at energy defects of 20–30 eV [31].

This implies that the cross sections for double charge exchange (O⁶⁺→O⁴⁺) measured by [24] should be largely attributed to autoionizing three electron capture reactions, rather than bound double electron capture reactions.

V. CONCLUSIONS

In the interaction between comets and the solar wind, collisions between the O⁶⁺ and water molecules play a key role. We have deduced velocity dependent state selective and total one electron capture cross sections for collisions between O⁶⁺ and H₂O, at collision energies between 0.11 and 7.5 keV/amu. These energies correspond to velocities typical for the solar wind, i.e., 150–1200 km s⁻¹.

Our results show that single electron capture mainly leads to population of the $n=4$ state and that the subsequent decay gives rise to strong euv emission between 10 and 20 nm. The relative strength of the different euv lines strongly depends on the collision velocity and might be used as a velocimetric diagnostic in comet-wind interactions, for example, by observing the ratio between the $1s^23d-1s^22p$ and $1s^24p-1s^22s$ transitions.

We also used our data to determine total one electron capture cross sections. From a comparison with other experimental studies, we conclude that pure one electron transfer constitutes only 60% of the total charge changing cross section, and that multiple electron processes thus play an important role in collisions between O⁶⁺ and H₂O. These results emphasize that a thorough understanding of charge exchange processes is of utmost importance for modeling of solar wind charge state distributions in cometary and planetary atmospheres.

ACKNOWLEDGMENTS

This work is part of the research program of the Stichting voor Fundamenteel Onderzoek der Materie (FOM) which is financially supported by the Stichting voor Nederlands Wetenschappelijk Onderzoek (NWO), and it is part of the research collaboration agreement between the Gesellschaft für Schwerionenforschung (GSI) and the University of Groningen (RuG).

- [1] C. M. Lisse, K. Dennerl, J. Englhauser, M. Harden, F. E. Marshall, M. J. Mumma, R. Petre, J. P. Pye, M. J. Ricketts, J. Schmitt, J. Trümper, and R. G. West, *Science* **274**, 205 (1996).
 [2] V. A. Krasnopolsky, M. J. Mumma, M. Abbott, B. C. Flynn, K. J. Meech, D. K. Yeomans, P. D. Feldman, and C. B. Cos-

movici, *Science* **277**, 1488 (1997).

- [3] K. Dennerl, C. M. Lisse, A. Bhardwaj, V. Burwitz, J. Englhauser, H. Gunell, M. Holmström, F. Jansen, V. Kharchenko, and P. M. Rodríguez-Pascal, *Astron. Astrophys.* **451**, 709 (2006).

- [4] C. M. Lisse, D. J. Christian, K. Dennerl, S. J. Wolk, D. Bodewits, R. Hoekstra, M. R. Combi, T. Mäkinen, M. Dryer, C. D. Fry, and H. Weaver, *Astrophys. J.* **635**, 1329 (2006).
- [5] V. A. Krasnopolsky *et al.*, *Icarus* **160**, 437 (2002).
- [6] T. E. Cravens, *Science* **296**, 1042 (2002).
- [7] V. Kharchenko, M. Rigazio, A. Dalgarno, and V. A. Krasnopolsky, *Astrophys. J. Lett.* **585**, L73 (2003).
- [8] P. Beiersdorfer, K. R. Boyce, G. V. Brown, H. Chen, S. M. Kahn, R. L. Kelley, M. May, R. E. Olson, F. S. Porter, C. K. Stahle, and W. A. Tillotson, *Science* **300**, 1558 (2003).
- [9] D. Bodewits, Z. Juhász, R. Hoekstra, and A. G. G. M. Tielens, *Astrophys. J. Lett.* **606**, 81 (2004).
- [10] N. A. Schwadron and T. E. Cravens, *Astrophys. J.* **544**, 558 (2000).
- [11] H. A. Weaver, P. D. Feldman, M. R. Combi, V. Krasnopolsky, C. M. Lisse, and D. E. Shemansky, *Astrophys. J. Lett.* **576**, L95 (2002).
- [12] V. A. Krasnopolsky and M. J. Mumma, *Astrophys. J.* **549**, 629 (2001).
- [13] J. H. Waite, Jr., F. Bagenal, F. Seward, C. Na, G. R. Gladstone, T. E. Cravens, K. C. Hurley, J. T. Clarke, R. Elsner, and S. A. Stem, *J. Geophys. Res.* **99**, 14799 (1994).
- [14] V. Kharchenko, W. Liu, and A. Dalgarno, *J. Geophys. Res.* **103**, 26687 (1998).
- [15] W. Liu and D. Schultz, *Astrophys. J.* **526**, 538 (1999).
- [16] D. Dijkkamp, Yu. S. Gordeev, A. Brazuk, A. G. Drentje, and F. J. de Heer, *J. Phys. (France) Lett.* **18**, 737 (1985).
- [17] W. Fritsch and C. D. Lin, *J. Phys. (France) Lett.* **19**, 2683 (1986).
- [18] N. Shimakura, H. Sato, M. Kimura, and T. Watanabe, *J. Phys. (France) Lett.* **20**, 1801 (1987).
- [19] J. P. M. Beijers, R. Hoekstra, A. R. Schlatmann, R. Morgenstern, and F. J. de Heer, *J. Phys. (France) Lett.* **25**, 463 (1992).
- [20] G. Lubinski, Z. Juhász, R. Morgenstern, and R. Hoekstra, *J. Phys. B* **33**, 5275 (2000).
- [21] D. Kearns, R. W. McCullough, R. Trassl, and H. B. Gilbody, *J. Phys. B* **36**, 3653 (2003).
- [22] D. Bodewits, R. W. McCullough, A. G. G. M. Tielens, and R. Hoekstra, *Phys. Scr.* **70**, C17 (2004).
- [23] S. Otranto, R. E. Olson, and P. Beiersdorfer, *Phys. Rev. A* **73**, 022723 (2006).
- [24] R. J. Mawhorter, A. Chutjian, T. E. Cravens, N. Djuric, S. Hossain, C. M. Lisse, J. A. MacAskill, S. J. Smith, J. Simic, and I. D. Williams, *Phys. Rev. A* **75**, 032704 (2007).
- [25] R. Hoekstra, F. J. de Heer, and R. Morgenstern, *J. Phys. B* **24**, 4025 (1991).
- [26] R. Hoekstra, J. P. M. Beijers, A. R. Schlatmann, R. Morgenstern, and F. J. de Heer, *Phys. Rev. A* **41**, 4800 (1990).
- [27] D. Bodewits, Ph.D. thesis, University of Groningen, 2007 (available up on request).
- [28] Z. D. Pesic, J.-Y. Chesnel, R. Hellhammer, B. Sulik, and N. Stolterfoht, *J. Phys. B* **37**, 1405 (2004).
- [29] B. Seredyuk, R. W. McCullough, H. Tawara, H. B. Gilbody, D. Bodewits, R. Hoekstra, A. G. G. M. Tielens, P. Sobocinski, D. Pesic, R. Hellhammer, B. Sulik, N. Stolterfoht, O. Abu-Haija, and E. Y. Kamber, *Phys. Rev. A* **71**, 022705 (2005).
- [30] D. Bodewits, R. Hoekstra, B. Seredyuk, R. W. McCullough, G. H. Jones, and A. G. G. M. Tielens, *Astrophys. J.* **642**, 593 (2006).
- [31] B. Seredyuk, R. W. McCullough, and H. B. Gilbody, *Phys. Rev. A* **72**, 022710 (2005).
- [32] A. Niehaus, *J. Phys. (France) Lett.* **19**, 2925 (1986).
- [33] R. K. Janev and H. Winter, *Phys. Rep.* **117**, 265 (1985).
- [34] G. Lubinski, Z. Juhász, R. Morgenstern, and R. Hoekstra, *Phys. Rev. Lett.* **86**, 616 (2001).
- [35] V. A. Abramov, F. F. Baryshnikov, and V. S. Lisitsa, *JETP Lett.* **27**, 464 (1978).
- [36] R. K. Janev, D. S. Belic, and B. H. Bransden, *Phys. Rev. A* **28**, 1293 (1983).
- [37] J. Burgdörfer, R. Morgenstern, and A. Niehaus, *J. Phys. (France) Lett.* **19**, L507 (1986).
- [38] J. B. Greenwood, I. D. Williams, S. J. Smith, and A. Chutjian, *Phys. Rev. A* **63**, 062707 (2001).
- [39] F. Alvarado, R. Hoekstra, and T. Schlathölter, *J. Phys. B* **38**, 4085 (2005).
- [40] S. Knoop, V. G. Hasan, R. Morgenstern, and R. Hoekstra, *Europhys. Lett.* **74**, 992 (2006).